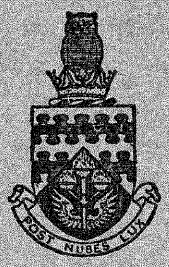

THE COLLEGE OF AERONAUTICS

CRANFIELD

THE FREE-MOLECULE FLOW CHARACTERISTICS OF CONCAVE SURFACES

by

M.J. Pratt

NOTE No. 155

June 1963

THE COLLEGE OF AERONAUTICS

CRANFIELD

The free-molecule flow characteristics of concave surfaces

- by -

M.J. Pratt, B.A., D.C.Ae.

CORRIGENDA

Page 8, Equation (6a) last term. For $d\underline{c}d\omega$ read $dcd\omega$

Page 11, Equation (15), for $2n_\infty(\xi)T\ F(\chi,S)$ read $2n_\infty(\xi)T_\infty F(\chi,S)$

Page 14, third equation of Equations (21) for $\frac{1}{2}A_B\rho_\infty U_\infty^2$ read $\frac{1}{2}A_B\rho_\infty U_\infty^3$

Page 18, Equation (29) for $\sqrt{\frac{RT_b}{2\pi}}$ read $\sqrt{\frac{2\pi}{RT_b}}$

Page 31, Table I, heading to first column for H read Θ.

NOTE NO. 155

June 1963

THE COLLEGE OF AERONAUTICS

CRANFIELD

The free-molecule flow characteristics of concave surfaces

- by -

M.J. Pratt, B.A., D.C.Ae.

SUMMARY

The problem of free-molecule flow over concave surfaces is investigated, and general equations formulated for the lift, drag, and heat transfer characteristics of such surfaces. The effect of multiple reflections is taken into account by use of the Clausing integral equation to determine the redistribution of molecular flux over the surface. It is assumed that emission of molecules from the surface is purely diffuse, and that the reflected molecules are perfectly accommodated to the surface conditions.

The equations obtained are solved for the cases of (i) an infinitely long circular cylindrical arc and (ii) a section of a spherical surface, at hyperthermal velocities. It is found that under the above conditions the local heat transfer characteristics are the same as those of the corresponding convex surface, the total heat transfer being independent of the geometry of the surface. As drag devices, the concave surfaces examined prove only slightly more effective than a flat plate at similar incidence, and as a generator of lift the cylindrically cambered plate is significantly inferior to the flat plate at similar incidence.

Table of contents

Notation

Roman symbols

A_B	base area of surface
$\underline{c}$	molecular velocity
c_x, c_y, c_z	cartesian components of $\underline{c}$
C_D	drag coefficient
C_L	lift coefficient
C_H	total heat transfer coefficient
D	total drag force
E_{int}	internal energy transfer rate to surface
E_{tr}	translational energy transfer rate to surface
$f(\underline{c})$	molecular velocity distribution function
F) G) H)	functions of (χ, S)
j	number of molecular degrees of freedom
K	kernel of integral equation
L	total lift force
m	molecular mass
n	molecular concentration (no. of molecules per unit volume)
N	molecular number flux
p	pressure
$\dot{Q}$	total heat transfer rate
r	radius of cylinder or sphere
r_{12}	distance between two surface elements

R	gas constant per gram of gas
S	molecular speed ratio = $U_\infty/\sqrt{2RT_\infty}$
T	temperature
U_∞	free-stream velocity
z	spanwise coordinate of cylindrical surface

Greek symbols

α	angle of incidence
α^*	$\pi/2 - \alpha$
α'	thermal accommodation coefficient
β	angle between free-stream and normal to surface
γ	ratio of specific heats
δ	angle between normal to surface and velocity vector of multiply reflected molecule
ϵ	parameter relating reflection components of aerodynamic coefficients to corresponding values for a flat plate at similar incidence
θ	polar coordinate of a point on the surface
Θ	limit on θ
λ	angle between $\underline{L}$ and lift vector at $\underline{\xi}$
$\underline{\xi}$	position vector of a point on the surface
ρ	gas density
Σ	area of the surface
τ	shear force per unit area
φ, ψ	polar coordinates centred at $\underline{\xi}$
Φ, Ψ	limits on φ, ψ
χ	$\sin\varphi \cos(\beta-\psi)$

ω	solid angle
Ω	limit on ω

Subscripts

i	relating to total number of incident molecules
∞	relating to free-stream molecules or conditions
b	relating to multiply reflected molecules or surface conditions
r	relating to total number of reflected molecules

Superscripts

(c)	relating to the cylindrical surface
(s)	relating to the spherical surface

1. Introduction

1.1 In gas flows at sufficiently low densities, the scale of molecular motion can become comparable to the size of bodies of practical interest in aerodynamic applications. When the density is so low that the effects of collisions between the gas molecules are far outweighed by the effects of collisions of the molecules with a body in the flow, we have the régime of free-molecule flow, first defined in 1934 by Zahm (1). The flow quantities are convected by the individual molecules rather than transferred by the intermediary of collisions, and concepts such as viscosity, which are intimately connected with intermolecular collision processes, entirely lose their significance. It is usual to define a free-molecule flow as a flow having a Knudsen number greater than about 10, where the Knudsen number is the ratio of the molecular mean free path-length to a typical dimension of a body in the flow.

In recent years the study of the aerodynamics of free-molecule flows has been stimulated by the practical possibilities of flight in the upper regions of the atmosphere. Numerous investigators have examined the aerodynamic characteristics of bodies of various configurations in free-molecule flows; an article by Schaaf and Chambré (2) conveniently tabulates references to some of this work. A comprehensive summary of the theory involved is given in a textbook by Patterson (3).

The majority of workers in this field have confined their attentions to bodies having surfaces which are either flat or convex, and comparatively little research has been concerned with non-convex configurations. Special problems arise in the treatment of such geometries owing to the occurrence of multiple molecular reflections. Hurlbut (4) has obtained some approximate results, while the following analysis is founded upon an outline by Cohen (5) of the approach to an exact method of solution. The present work presents an analysis of two classes of concave surfaces, from which solutions for the lift, drag, and heat transfer are obtained. At a late stage in the preparation of this work, two articles by Chahine (6,7) were published, covering much the same ground, although the results given are not entirely in agreement with those obtained here. The present analysis appears to have certain advantages over the method used by Chahine, notably in the treatment of axisymmetric surfaces.

2. Analysis

2.1 Preliminary

The total momentum and energy transfer to a body in free-molecule flow arises from two components. Firstly, momentum and energy are yielded up to the body by the incident molecules, and secondly, momentum and energy are transported away from the body by the reflected molecules. Since the molecular mean free path is large compared with the body dimensions, the incident and reflected flows can be taken as separate and non-interacting. The precise nature of the reflection of molecules from the

surface is at present still imperfectly understood, but a concise summary of the present state of knowledge is given by Charwat (8). In the following analysis a number of assumptions are made concerning the reflection process:

(i) The reflection is perfectly diffuse. This condition implies that the incident molecules are adsorbed by the surface and later re-emitted with a Maxwellian velocity distribution. The reflected molecules obey Lambert's cosine law of diffuse reflection.

(ii) The velocity distribution corresponds to the temperature of the emitting surface (i.e. perfect accommodation occurs at the surface).

(iii) No surface poisoning or trapping of molecules occurs at the surface.

Experimentally it is found (9) that for air on 'engineering' surfaces (which by molecular standards are 'dirty' due to oxidation and adsorption of gases) these three conditions are fulfilled fairly well, although work by Roberts (10) has shown that the situation can be drastically altered in certain cases involving clean surfaces. He finds, for instance, that the reflection of helium atoms from a clean tungsten surface is almost completely specular. This effect is apparently due to the fact that the de Broglie wavelength of the incident atoms is comparable with the lattice spacing of the tungsten surface. However, here it will be assumed that we are dealing with 'engineering' surfaces.

The further assumptions will be made that:

(iv) The gas stream consists of a single molecular species.

(v) The surface temperature is constant over the surface and invariant with time.

(vi) The surface temperature is sufficiently high to avoid 'cold wall paradoxes' (11). This condition stipulates that the re-emitted molecules must have sufficient velocity to avoid large increases in gas density building up at the surface, which may lead to violation of the conditions defining a free-molecule flow.

2.2 The molecular flux at the surface

The total incident molecular flux at a point $\underline{\xi}_1$ on a concave surface is given by

$$N_i(\underline{\xi}_1) = N_\infty(\underline{\xi}_1) + N_b(\underline{\xi}_1), \qquad (1)$$

where N_∞ is the flux of free-stream molecules and N_b the flux of multiply reflected molecules from the remainder of the surface.

In the case of a non-concave surface the term $N_b(\underline{\xi}_1)$ is zero; it is this multiple reflection term which gives rise to the additional complications inherent in the theory of the concave surface. If we consider the number of molecules emitted per unit time by a surface element $d\Sigma_2$ at $\underline{\xi}_2$ and intercepted by $d\Sigma_1$ at $\underline{\xi}_1$ we obtain, using the cosine law of reflection,

$$dN_b(\underline{\xi}_1)d\Sigma_1 = \frac{\cos\delta_1 \cos\delta_2}{\pi r_{12}^2} N_r(\underline{\xi}_2)d\Sigma_1\, d\Sigma_2, \qquad (2)$$

in which the symbols are defined in Figure 1. Since $N_i(\underline{\xi}_2) = N_r(\underline{\xi}_2)$ from assumption (iii), we obtain from equations (1) and (2)

$$N_i(\underline{\xi}_1) = N_\infty(\underline{\xi}_1) + \int_{\Sigma_2} K(\underline{\xi}_1, \underline{\xi}_2)N_i(\underline{\xi}_2)d\Sigma_2, \qquad (3)$$

in which $K(\underline{\xi}_1, \underline{\xi}_2) = \dfrac{\cos\delta_1 \cos\delta_2}{\pi r_{12}^2}$.

Equation (3) is a Fredholm integral equation of the second type, in which the kernel is seen to be symmetrical. This type of problem was first formulated in terms of an integral equation in 1929 by Clausing (12), who was concerned with the flow of rarefied gases through pipes.

2.3 Mass, momentum and energy fluxes at the surface

Using the coordinate system defined in Figure 2, the free-stream molecular flux incident on a non-concave surface at the point $\underline{\xi}$ is given by

$$N_\infty(\underline{\xi}) = \int_{-\infty}^{\infty}\int_{-\infty}^{\infty}\int_{0}^{\infty} c_x f(\underline{c})dc_x dc_y dc_z,$$

where $f(\underline{c})$ is a velocity distribution function whose significance is explained in any textbook on the kinetic theory of cases (for example that by Kennard (13)).

The lower limit of zero on c_x implies that molecules having negative x-velocities cannot strike the surface at $\underline{\xi}$. This equation may be

rewritten in spherical polar coordinates as

$$N_\infty(\underline{\xi}) = \iint_{2\pi} \sin\varphi\cos\psi \int_0^\infty c^3 f(\underline{c})\,dc\,d\omega \qquad (4)$$

where $c_x = c\sin\varphi\cos\psi$

$dc_x\,dc_y\,dc_z = c^2\sin\varphi\,d\varphi\,d\psi\,dc$

$d\omega = \sin\varphi\,d\varphi\,d\psi$.

In the case of the concave surface, however, only those free-stream molecules travelling in directions included in the solid angle Ω_1 subtended by the boundary of the surface at $\underline{\xi}$ can actually strike the surface at $\underline{\xi}$. Moreover, a further contribution to the total molecular flux arises from impacts at $\underline{\xi}$ of molecules reemitted from other parts of the surface, whose velocities will be confined to the solid angle Ω_2 subtended at $\underline{\xi}$ by the surface itself. Thus we obtain the equation

$$N_i(\underline{\xi}) = N_\infty(\underline{\xi}) + N_b(\underline{\xi})$$

$$= \iint_{\Omega_1} \sin\varphi\cos\psi \int_0^\infty c^3 f_1(\underline{c})\,dc\,d\omega + \iint_{\Omega_2} \sin\varphi\cos\psi \int_0^\infty c^3 f_2(\underline{c})\,dc\,d\omega \qquad (5)$$

Here $f_1(\underline{c})$ is a Maxwellian velocity distribution function corresponding to the free-stream temperature T_∞, and including the superimposed free-stream velocity U_∞. The function $f_2(\underline{c})$ is a Maxwellian velocity distribution function for a gas at rest with respect to the surface, corresponding to the surface temperature T_b.

In the case of momentum and energy fluxes at the surface we have three contributions: (a) from incident free-stream molecules, (b) from incident multiply reflected molecules, and (c) from reemissions of molecules at $\underline{\xi}$. These latter are emitted isotropically with a distribution function $f_3(\underline{c})$ corresponding to the surface temperature T_b, within the solid angle $\Omega_3 = \Omega_1 + \Omega_2 = 2\pi$. The cartesian expressions have the forms

Normal momentum flux (pressure) $\quad p = m\iiint c_x^2 f(\underline{c})\,d\underline{c}$

Tangential momentum flux (shear) $\tau = m\iiint c_x c_y f(\underline{c})d\underline{c}$

Translational energy flux $E_{tr} = \frac{m}{2}\iiint c_x(\underline{c}.\underline{c})f(\underline{c})d\underline{c}$

We are led to the following expressions for the pressure, shear, and translational energy flux at $\underline{\xi}$.

$$p(\underline{\xi}) = m\iint_{\Omega_1}\sin^2\varphi\cos^2\psi\int_0^\infty c^4 f_1(\underline{c})dcd\omega + m\iint_{\Omega_2}\sin^2\varphi\cos^2\psi\int_0^\infty c^4 f_2(\underline{c})dcd\omega$$

$$+ m\iint_{\Omega_3}\sin^2\varphi\cos^2\psi\int_0^\infty c^4 f_3(\underline{c})d\underline{c}d\omega \qquad (6a)$$

$$\tau(\underline{\xi}) = m\iint_{\Omega_1}\sin^2\varphi\cos\psi\sin\psi\int_0^\infty c^4 f_1(\underline{c})dcd\omega + m\iint_{\Omega_2}\sin^2\varphi\cos\psi\sin\psi\int_0^\infty c^4 f_2(\underline{c})dcd\omega$$

$$+ m\iint_{\Omega_3}\sin^2\varphi\cos\psi\sin\psi\int_0^\infty c^4 f_3(\underline{c})dcd\omega \qquad (6b)$$

$$E_{tr}(\underline{\xi}) = \frac{m}{2}\iint_{\Omega_1}\sin\varphi\cos\psi\int_0^\infty c^5 f_1(\underline{c})dcd\omega + \frac{m}{2}\iint_{\Omega_2}\sin\varphi\cos\psi\int_0^\infty c^5 f_2(\underline{c})dcd\omega$$

$$- \frac{m}{2}\iint_{\Omega_3}\sin\varphi\cos\psi\int_0^\infty c^5 f_3(\underline{c})dcd\omega \qquad (6c)$$

In fact the last term in equation (6b) vanishes on integration because of isotropic reemission, the contribution to shear at the surface arising from reemitted molecules is zero.

In calculating the heat transfer rate we must include also the effect of internal degrees of freedom of the molecules, in the case of gases which are not monatomic. Assuming equipartition of energy, each molecule carries internal energy $\frac{1}{2}mRj_{int}T$, where j_{int} is the number of internal degrees of freedom. For a perfect gas $j_{total} = 3 + j_{int}$, and $j_{total} = 2/(\gamma - 1)$, giving $j_{int} = (5 - 3\gamma)/(\gamma - 1)$. The internal energy transfer is then, from equation (1)

$$E_{int}(\underline{\xi}) = \left(\frac{5-3\gamma}{\gamma-1}\right)\frac{mR}{2}\left\{N_\infty T_\infty + N_b T_b - N_r T_b\right\}$$

$$= \left(\frac{5-3\gamma}{\gamma-1}\right)\frac{mR}{2} N_\infty(\underline{\xi})\left\{T_\infty - T_b\right\} \qquad (7)$$

2.4 Drag, lift and heat transfer rate of the surface

When an element $d\Sigma$ of the surface is inclined so that its normal makes an angle β with the free-stream direction, its drag is

$$dD = d\Sigma(p\cos\beta + \tau\sin\beta) \qquad (8a)$$

Similarly, a perpendicular lift force

$$dL = d\Sigma(p\sin\beta - \tau\cos\beta) \qquad (8b)$$

will exist, acting in the plane containing the free-stream direction and the normal to the surface. Using equations (6) and (8a), the total drag of the entire surface becomes

$$D = \int_\Sigma (p\cos\beta + \tau\sin\beta)d\Sigma$$

$$= m\int_\Sigma \Bigg\{ \Bigg[\iint_{\Omega_1} \sin^2\varphi\cos^2\psi \int_0^\infty c^4 f_1(\underline{c})dcd\omega + \iint_{\Omega_2} \sin^2\varphi\cos^2\psi \int_0^\infty c^4 f_2(\underline{c})dcd\omega$$

$$+ \iint_{\Omega_1} \sin^2\varphi\cos^2\psi \int_0^\infty c^4 f_3(\underline{c})dcd\omega + \iint_{\Omega_2} \sin^2\varphi\cos^2\psi \int_0^\infty c^4 f_3(\underline{c})dcd\omega \Bigg]\cos\beta$$

$$+ \Bigg[\iint_{\Omega_1} \sin^2\varphi\sin\psi\cos\psi \int_0^\infty c^4 f_1(\underline{c})dcd\omega + \iint_{\Omega_2} \sin^2\varphi\sin\psi\cos\psi \int_0^\infty c^4 f_2(\underline{c})dcd\omega$$

$$+ \iint_{\Omega_1} \sin^2\varphi\cos\psi\sin\psi \int_0^\infty c^4 f_3(\underline{c})dcd\omega + \iint_{\Omega_2} \sin^2\varphi\cos\psi\sin\psi \int_0^\infty c^4 f_3(\underline{c})dcd\omega \Bigg]\sin\beta \Bigg\} d\Sigma \qquad (9)$$

In the above relation the integrals over Ω_3 in equations (6) have been written as the sum of integrals over Ω_1 and Ω_2. The second and sixth terms, taken together, represent the drag of the surface due to impacts

of multiply reflected molecules, while the fourth and eighth terms give the drag due to reemissions of molecules which are, however, destined to encounter the surface once more. These four terms, then, describe a momentum transfer which is purely an internal process, and cannot contribute to the total drag of the surface. The only events significant in this connection are (i) impacts of free-stream molecules, and (ii) reemissions of molecules into the free-stream, carrying momentum completely away from the body. We may ignore the even-numbered terms in equation (9), and rewrite it as

$$D = m\int_{\Sigma}\iint_{\Omega_1} \sin^2\varphi\left\{\cos^2\psi\cos\beta + \cos\psi\sin\psi\sin\beta\right\}\int_0^{\infty} c^4\left[f_1(\underline{c}) + f_3(\underline{c})\right]dc\,d\omega\,d\Sigma \tag{10}$$

while similar expressions may be found for the lift and heat transfer.

The velocity distribution function for the reemitted molecules is assumed to have the Maxwellian form

$$f_3(\underline{c}) = \frac{n_r(\underline{\xi})}{(2\pi R\,T_b)^{3/2}}\, e^{-\frac{c^2}{2RT_b}} \tag{11}$$

in which $n_r(\underline{\xi})$ is the molecular concentration of emitted particles at $\underline{\xi}$. It may be shown (vide, for instance, ref. (11), p. 401) that n_r and N_r are related by

$$n_r(\underline{\xi}) = N_r(\underline{\xi})\Big/\sqrt{\frac{RT_b}{2\pi}}\,, \tag{12}$$

$$= N_i(\underline{\xi})\Big/\sqrt{\frac{RT_b}{2\pi}}$$

from condition (iii). Using equation (11) we now find

$$\int_0^{\infty} c^4 f_3(\underline{c})dc = \int_0^{\infty} \frac{n_r(\underline{\xi})c^4}{(2\pi RT_b)^{3/2}}\, e^{-\frac{c^2}{2RT_b}}\, dc = \frac{3}{4\pi}\, n_r(\underline{\xi})RT_b \tag{13}$$

on evaluation of the standard integral.

The velocity distribution function for the free-stream molecules is also Maxwellian, but includes the free-stream velocity U_∞

$$f_1(\underline{c}) = \frac{n_\infty(\underline{\xi})}{(2R\pi T_\infty)^{3/2}} e^{-\frac{1}{2RT_\infty}\{(c_x - U_\infty\cos\beta)^2+(c_y - U_\infty\sin\beta)^2+ c_z^2\}}$$

$$= \frac{n_\infty(\underline{\xi})}{(2\pi RT_\infty)^{3/2}} e^{-\frac{1}{2RT_\infty}\{c^2 - 2cU_\infty\sin\varphi\cos(\beta-\psi)+ U_\infty^2\}} \qquad (14)$$

From this we obtain

$$\int_0^\infty c^4 f_1(\underline{c})dc = \frac{2}{\pi} n_\infty(\underline{\xi})RT_\infty F(\chi,S)$$

Here $\chi = \sin\varphi\cos(\beta-\psi)$ and $S = U_\infty/\sqrt{2RT_\infty}$, the ratio of the free-stream velocity to the most probable molecular velocity, an important parameter in free-molecule flow theory which is known as the speed ratio. $F(\chi,S)$ represents the expression

$$F(\chi,S) = \left\{\frac{3}{8} + \frac{3}{2}\chi^2S^2 + \frac{1}{2}\chi^4S^4\right\}\left\{1 + \mathrm{erf}(\chi S)\right\}e^{-S^2(1-\chi^2)} + \left\{\frac{5}{4}\chi S + \frac{1}{2}\chi^3S^3\right\}\frac{e^{-S^2}}{\sqrt{\pi}}$$

Finally, the expression for the total drag becomes

$$D = \frac{mR}{\pi}\int_\Sigma\iint_{\Omega_1}\sin^2\varphi\cos\psi\cos(\beta-\psi)\left\{\frac{3}{4}n_r(\underline{\xi})T_b + 2n_\infty(\underline{\xi})T F(\chi,S)\right\}d\omega d\Sigma \qquad (15)$$

By a similar process the lift is given by

$$L = \frac{mR}{\pi}\int_\Sigma\iint_{\Omega_1}\sin^2\varphi\cos\psi\sin(\beta-\psi)\left\{\frac{3}{4}n_r(\underline{\xi})T_b + 2n_\infty(\underline{\xi})T_\infty F(\chi,S)\right\}\cos\lambda(\underline{\xi})d\omega d\Sigma \qquad (16)$$

The angle λ is that between the lift-vector of the surface element $d\Sigma$ at ξ and the direction in which the total lift is taken to act. In general there will also be a transverse force, perpendicular both to the drag and the lift, whose value is given by equation (16) with the substitution of $\sin\lambda$ for $\cos\lambda$. Here we will deal only with surfaces which are symmetrical about a plane containing the free-stream direction; the lift is taken to act in the plane of symmetry and the transverse force is then zero.

For the translational energy transfer, we obtain from equation (6c)

$$E_{tr} = \frac{m}{2}\int_{\Sigma}\iint_{\Omega_1} \sin\varphi\cos\psi \int_0^{\infty} c^5[f_1(\underline{c}) - f_3(\underline{c})]dcd\omega d\Sigma \tag{17}$$

Equation (7) may be rewritten in the form

$$E_{int}(\underline{\xi}) = \left(\frac{5 - 3\gamma}{\gamma - 1}\right)\frac{mR}{2}\left\{T_\infty\iint_{\Omega_1}\sin\varphi\cos\psi\int_0^{\infty} c^3 f_1(\underline{c})dcd\omega\right.$$

$$+ T_b\iint_{\Omega_2}\sin\varphi\cos\psi\int_0^{\infty} c^3 f_2(\underline{c})dcd\omega - T_b\iint_{\Omega_1}\sin\varphi\cos\psi\int_0^{\infty} c^3 f_3(\underline{c})dcd\omega$$

$$\left. - T_b\iint_{\Omega_2}\sin\varphi\cos\psi\int_0^{\infty} c^3 f_3(\underline{c})dcd\omega\right\}$$

We may cancel the second and fourth terms, which describe a purely internal process, to find for the transfer of internal energy

$$E_{int} = \frac{mR}{2}\left(\frac{5 - 3\gamma}{\gamma - 1}\right)\int_{\Sigma}\iint_{\Omega_1}\sin\varphi\cos\psi\int_0^{\infty} c^3[T_\infty f_1(\underline{c}) - T_b f_3(\underline{c})]dcd\omega d\Sigma \tag{18}$$

Combining these two equations and integrating, we find for the total convective heat transfer rate to the surface

$$\dot{Q} = \int_{\Sigma}\iint_{\Omega_1}\sin\varphi\cos\psi\left\{\left(\frac{2RT_\infty}{\pi}\right)^{3/2} n_\infty(\underline{\xi})\left[G(\chi,S) + \frac{1}{2}\left(\frac{5 - 3\gamma}{\gamma - 1}\right)H(\chi,S)\right]\right.$$

$$\left. - \left(\frac{2RT_b}{\pi}\right)^{3/2} n_r(\underline{\xi}) \cdot \frac{1}{4}\left(\frac{\gamma + 1}{\gamma - 1}\right)\right\}d\omega d\Sigma, \tag{19}$$

in which

$$G(\chi,S) = \left\{\frac{15}{8}\chi S + \frac{5}{2}\chi^3 S^3 + \frac{1}{2}\chi^5 S^5\right\}\left\{1 + \mathrm{erf}(\chi S)\right\}\sqrt{\pi}\, e^{-S^2(1-\chi^2)}$$

$$+ \left\{1 + \frac{9}{4}\chi^2 S^2 + \frac{1}{2}\chi^4 S^4\right\}e^{-S^2}$$

and

$$H(\chi,S) = \left\{\frac{3}{4}\chi S + \frac{1}{2}\chi^3 S^3\right\}\left\{1 + \mathrm{erf}(\chi S)\right\}\sqrt{\pi}\, e^{-s^2(1-\chi^2)}$$

$$+ \left\{\frac{1}{2} + \frac{1}{2}\chi^2 S^2\right\} e^{-s^2}.$$

The analysis so far is completely general, and the expressions given for the drag, lift, and heat transfer by equations (15), (16) and (19) are valid for any surface, whether concave or not. For non-concave surfaces certain simplifications arise, since $\Omega_1 = 2\pi$ and $n_\infty(\underline{\xi}) = n_r(\underline{\xi})$.

2.5 The hyperthermal approximation

Most cases of practical interest, for instance satellites, many of which at present have orbits in the free-molecule flow region of the atmosphere, are concerned with speed ratios greater than about 6. We see that in such cases the exponential term in equations (15), (16) and (19) has its maximum value for $\chi = 1$, becoming very small as $\chi \to 0$. The functions $F(\chi,S)$, $G(\chi,S)$ and $H(\chi,S)$ also have their smallest value for $\chi = 0$. Since $\chi = \sin\phi\cos(\beta-\psi)$, this implies that by far the greatest contribution to D, L, and $\dot{Q}$ is due to molecules approaching each surface element $d\Sigma$ in a small solid angle about the free-stream direction. This is to be expected, since the free-stream velocity is considerably greater than the average molecular thermal velocity. It has been found (14) that for $S > 6$ the thermal velocities may justifiably be ignored in comparison with the free-stream velocity. This is known as the hyperthermal approximation, and leads to a considerable simplification in the theory.

In effect we now assume that each incident free-stream molecule impinges on the surface travelling in the free-stream direction with velocity U_∞. The total drag due to incidences of free-stream molecules (i.e. the momentum they transport to the surface per unit time) is then seen to be simply $A_B\rho_\infty U_\infty^2$, where A_B is the base area of the surface. Since no molecule carries momentum perpendicular to the free-stream the lift due to the incident molecules is zero, while the translational energy they transfer to the surface is $\frac{1}{2}A_B\rho_\infty U_\infty^3$. The internal energy transfer varies as U_∞, and may be neglected by comparison with the translational energy transfer. We shall assume that the velocity of reemission of molecules from the surface is sufficiently large that the reflected molecules contribute appreciably to D, L, and $\dot{Q}$. We thus replace those terms representing the contributions of the incident free-stream molecules in equations (15), (16) and (19) by the simpler expressions given above, which yields

$$D = A_B\rho_\infty U_\infty^2 + \frac{3RT_b}{4\pi}\int_\Sigma\int_{\Phi_1}^{\Phi_2}\int_{-\Psi_1}^{\Psi_2}\sin^3\varphi\cos\psi\cos(\beta-\psi).\rho_r(\underline{\xi})\,d\psi\,d\varphi\,d\Sigma$$

$$L = \frac{3RT_b}{4\pi}\int_\Sigma\int_{\Phi_1}^{\Phi_2}\int_{-\Psi_1}^{\Psi_2}\sin^3\varphi\cos\psi\sin(\beta-\psi)\rho_r(\underline{\xi})\cos\lambda(\underline{\xi})\,d\psi\,d\varphi\,d\Sigma \qquad (20)$$

$$\dot{Q} = \frac{1}{2}A_B\rho_\infty U_\infty^3 - \frac{1}{8}\left(\frac{\gamma+1}{\gamma-1}\right)\left(\frac{2RT_b}{\pi}\right)^{3/2}\int_\Sigma\int_{\Phi_1}^{\Phi_2}\int_{-\Psi_1}^{\Psi_2}\sin^2\varphi\cos\psi.\rho_r(\underline{\xi})\,d\psi\,d\varphi\,d\Sigma$$

where $\rho_r(\underline{\xi}) = mn_r(\underline{\xi})$, the density of reemitted gas at $\underline{\xi}$, and we have written $d\omega = \sin\varphi d\varphi d\psi$. We see that the lift developed by the surface is due entirely to the effect of reemissions.

2.6 Symmetrical surfaces

We may now perform the integration over φ. The surfaces to be considered will be (a) infinite cylindrical surfaces, with generators normal to the free-stream, and (b) surfaces axially symmetric about the free-stream direction. In either case, $\varphi = \pi/2$ represents a plane of symmetry, and hence the limits on φ are related by $\Phi_2 = \pi - \Phi_1$. Equations (20) now lead to

$$D = A_B\rho_\infty U_\infty^2 + \frac{3RT_b}{2\pi}\int_\Sigma\int_{-\Psi_1}^{\Psi_2}\rho_r(\underline{\xi})\cos\psi\cos(\beta-\psi)\{\cos\Phi_1 - \tfrac{1}{3}\cos^3\Phi_1\}\,d\psi\,d\Sigma$$

$$L = \frac{3RT_b}{2\pi}\int_\Sigma\int_{-\Psi_1}^{\Psi_2}\rho_r(\underline{\xi})\cos\psi\sin(\beta-\psi)\{\cos\Phi_1 - \tfrac{1}{3}\cos^3\Phi_1\}\cos\lambda(\underline{\xi})\,d\psi\,d\Sigma$$

$$\dot{Q} = \frac{1}{2}A_B\rho_\infty U_\infty^2 - \frac{1}{2}\left(\frac{\gamma+1}{\gamma-1}\right)\left(\frac{RT_b}{2\pi}\right)^{3/2}\int_\Sigma\int_{-\Psi_1}^{\Psi_2}\rho_r(\underline{\xi})\cos\psi\{\pi - 2\Phi_1 + \sin2\Phi_1\}\,d\psi\,d\Sigma \qquad (21)$$

In the above, ρ_r and λ are functions of the surface co-ordinates, and in general for concave surfaces $\Phi_1 = \Phi_1(\psi,\underline{\xi})$. For non-concave surfaces, $\Phi_1 = 0$ and the limits on ψ are $\pm\pi/2$.

In order to perform the ψ - integration we must determine the ψ - dependence of Φ_1, which entails specifying the nature of the surface to a greater extent.

2.7 General infinite cylindrical surfaces

The problem of the cylindrical surface of finite span is three-dimensional, due to the occurrence of end-effects. A simplification to two dimensions is obtained by taking the span of the surface as being infinite, when all variables become independent of the spanwise co-ordinate. The lift, drag, and heat transfer coefficients can then be ascertained per unit length of the surface.

Strictly speaking, in taking one dimension of the surface as infinite we are violating one of the restrictive conditions defining a free-molecule flow. Reemitted molecules travelling nearly parallel to the spanwise direction, since their mean free path is finite, will certainly undergo collisions in the vicinity of the surface, either with other reemitted molecules or with free-stream molecules. The incident and reflected flows are thus interacting. The foregoing objection may be overcome, however, by applying the results obtained for the infinite surface to a surface having the same cross-section but finite span. This span must be sufficiently large compared with the chord that end-effects may be neglected, but not so large compared with the mean free path of the reemitted molecules that the free-molecule flow conditions are infringed. The results of Sections 2.8 and 2.10 are valid within these limitations.

For the general infinite cylindrical surface with parallel generators normal to the flow $\Phi_1 = 0$, and since the lift contributions from each surface element act parallel and in planes of symmetry, $\lambda = 0$. Integration over ψ now yields

$$D = A_B \rho_\infty U_\infty^2 + \frac{RT_b}{2\pi} \int_\Sigma \rho_r(\underline{\xi}) \left\{ \cos\beta(\Psi_2+\Psi_1) + \sin(\Psi_2+\Psi_1)\cos(\Psi_2-\Psi_1-\beta) \right\} d\Sigma$$

$$L = \frac{RT_b}{2\pi} \int_\Sigma \rho_r(\underline{\xi}) \left\{ \sin\beta(\Psi_2+\Psi_1) - \sin(\Psi_2+\Psi_1)\sin(\Psi_2-\Psi_1-\beta) \right\} d\Sigma$$

$$\dot{Q} = \frac{1}{2} A_B \rho_\infty U_\infty^3 - \pi \left(\frac{\gamma+1}{\gamma-1}\right) \left(\frac{RT_b}{2\pi}\right)^{3/2} \int_\Sigma \rho_r(\underline{\xi}) \sin\tfrac{1}{2}(\Psi_2+\Psi_1)\cos\tfrac{1}{2}(\Psi_2-\Psi_1) d\Sigma \qquad (22)$$

Integration over the surface Σ now involves specifying Ψ_1, Ψ_2 and

ρ_r as functions of the surface co-ordinates. To find ρ_r the Clausing integral equation (3) must be solved; the simplest case is that of the circular cylindrical surface.

2.8 The infinite circular cylindrical arc

This surface, with its co-ordinate system, is shown in Figure 3. We shall deal first with the case where the chord of the arc is normal to the flow. The analysis is restricted to values of Θ between 0 and $\pi/2$, so that no part of the surface is shielded from the free-stream. Then in equations (22) the following relationships hold

$$\Psi_1 = \tfrac{1}{2}(\pi - \Theta - \theta),$$

$$\Psi_2 = \tfrac{1}{2}(\pi - \Theta + \theta),$$

$$\beta = \theta,$$

substitution yielding (per unit length of the surface)

$$D = A_B\rho_\infty U_\infty^2 + \frac{RT_b}{2\pi}\int_{-\Theta}^{\Theta}\rho_r(\theta)\left\{(\pi - \Theta)\cos\theta + \sin\Theta\right\}r\,d\theta$$

$$L = \frac{RT_b}{2\pi}\int_{-\Theta}^{\Theta}\rho_r(\theta)(\pi - \Theta)\sin\theta\,.\,r\,d\theta \qquad (23)$$

$$\dot{Q} = \tfrac{1}{2}A_B\rho_\infty U_\infty^3 - \pi\left(\frac{\gamma+1}{\gamma-1}\right)\left(\frac{RT_b}{2\pi}\right)^{3/2}\int_{-\Theta}^{\Theta}\rho_r(\theta)\cos\tfrac{1}{2}\theta\cos\tfrac{1}{2}\Theta\,.\,r\,d\theta$$

Since the surface has infinite span, ρ_r is a function of θ only.

In order to carry out the integration over θ, it remains to determine $\rho_r(\theta)$, which entails solving the Clausing equation (3). The kernel of the equation proves to be in this case

$$K_1 = \frac{\cos\delta_1\cos\delta_2}{\pi r_{12}^2} = \frac{4r^2\sin^4\tfrac{1}{2}|\theta_1-\theta_2|}{\pi\{(z_2-z_1)^2+4r^2\sin^2\tfrac{1}{2}|\theta_1-\theta_2|\}^2},$$

and hence we have

$$N_i(\theta_1) = N_\infty(\theta_1) + \int_{-\infty}^{\infty}\int_{-\Theta}^{\Theta}K_1(\theta_1,\theta_2,z_1,z_2)N_i(\theta_2)r\,d\theta_2\,dz_2.$$

The integration over z_2 is effected by a trigonometrical substitution to give

$$N_i(\theta_1) = N_\infty(\theta_1) + \frac{1}{4}\int_{-\Theta}^{\Theta} N_i(\theta_2)\sin\tfrac{1}{2}|\theta_1-\theta_2|\,d\theta_2 \qquad (24)$$

In this form the equation has a degenerate kernel, and the standard method of solution is to express the relation as a pair of linear simultaneous equations which may be solved in a straightforward manner (15). Alternatively, $N_i(\theta)$ may be expressed as a Fourier series

$$N_i(\theta_1) = a_o + \sum_{n=1}^{\infty} a_n \cos n\theta_1,$$

the coefficients a_n being determined in the usual manner by substitution into equation (24). However, in the present case a solution is obtained most conveniently by differentiating equation (24) twice with respect to θ_1. Care must be exercised in that although $\sin\frac{1}{2}|\theta_1-\theta_2|$ is continuous for $-\Theta \leqslant \theta_1 \leqslant \Theta$, its first derivative is not.

The number of free-stream molecules incident per second per unit area of surface is given simply by $N_\infty(\theta_1) = n_\infty U_\infty \cos\theta_1$ (volume swept out/second × particle concentration)$_\infty$, and we thus have

$$N_i(\theta_1) = n_\infty U_\infty \cos\theta_1 + \frac{1}{4}\int_{-\Theta}^{\theta} N_i(\theta_2)\sin\tfrac{1}{2}(\theta_1-\theta_2)d\theta_2 + \frac{1}{4}\int_{\theta}^{\Theta} N_i(\theta_2)\sin\tfrac{1}{2}(\theta_2-\theta_1)d\theta_2$$

Differentiation twice gives

$$\frac{d^2N_i(\theta_1)}{d\theta_1^2} = -n_\infty U_\infty \cos\theta_1 - \frac{1}{16}\int_{-\Theta}^{\theta} N_i(\theta_2)\sin\tfrac{1}{2}(\theta_1-\theta_2)d\theta_2 + \frac{1}{8}N_i(\theta_1)$$

$$-\frac{1}{16}\int_{\theta}^{\Theta} N_i(\theta_2)\sin\tfrac{1}{2}(\theta_2-\theta_1)d\theta_2 + \frac{1}{8}N_i(\theta_1)$$

$$= -n_\infty U_\infty \cos\theta_1 - \frac{1}{16}\int_{-\Theta}^{\Theta} N_i(\theta_2)\sin\tfrac{1}{2}|\theta_1-\theta_2|\,d\theta_2 + \frac{1}{4}N_i(\theta_1). \qquad (25)$$

The integral term may be eliminated between equations (24) and (25) to give the simple differential equation

$$\frac{d^2N_i(\theta_1)}{d\theta_1^2} = -\frac{3}{4} n_\infty U_\infty \cos\theta_1, \tag{26}$$

whose solution is of the form

$$N_i(\theta_1) = \frac{3}{4} n_\infty U_\infty \cos\theta_1 + B\theta_1 + C, \tag{27}$$

in which the constants B and C are determined from the boundary conditions by substitution of this solution back into equation (24). We find

$$B = 0, \quad C = \frac{1}{4} n_\infty U_\infty (2 - \cos\Theta).$$

The complete solution of the Clausing equation is thus

$$N_i(\theta) = n_\infty U_\infty \left[\frac{3}{4}\cos\theta + \frac{1}{4}(2 - \cos\Theta)\right] \tag{28}$$

Equation (12) may now be used to give

$$\rho_r(\theta) = \rho_\infty U_\infty \sqrt{\frac{RT_b}{2\pi}} \left[\frac{3}{4}\cos\theta + \frac{1}{4}(2 - \cos\Theta)\right], \tag{29}$$

which expression must be substituted into equations (23). Evaluation of the resulting integrals gives

$$D = A_B \rho_\infty U_\infty^2 + \rho_\infty U_\infty r \sqrt{\frac{RT_b}{2\pi}} \left\{(\pi - \Theta)\left[\frac{3}{4}\Theta + \sin\Theta + \frac{1}{4}\sin\Theta\cos\Theta\right]\right.$$

$$\left. + \sin\Theta\left[\Theta + \frac{3}{2}\sin\Theta - \frac{1}{2}\Theta\cos\Theta\right]\right\}$$

$$L = 0 \tag{30}$$

$$\dot{Q} = \tfrac{1}{2} A_B \rho_\infty U_\infty^3 \qquad - \rho_\infty U_\infty r RT_b \left(\frac{\gamma+1}{\gamma-1}\right)\sin\Theta$$

These results are reduced to coefficient form with reference to the base area per unit length, $A_B = 2\ r \sin\Theta$ (the heat transfer coefficient C_H is here defined as $C_H = \dot{Q}/\tfrac{1}{2} A_B \rho_\infty U_\infty^3$).

We find

$$C_D = 2 + \epsilon_D^{(c)}(\Theta)\,\frac{\sqrt{\pi}}{S}\sqrt{\frac{T_b}{T_\infty}}$$

$$C_L = 0, \qquad (31)$$

$$C_H = 1 - \tfrac{1}{2}\left(\frac{\gamma+1}{\gamma-1}\right)\frac{T_b}{T_\infty}\cdot\frac{1}{S^2}$$

where in equation (31)

$$\epsilon_D^{(c)}(\Theta) = \frac{1}{2\pi}\left\{(\pi - \Theta)\left[1 + \frac{1}{4}\cos\Theta + \frac{3}{4}\frac{\Theta}{\sin\Theta}\right] + \left[\Theta + \frac{3}{2}\sin\Theta - \tfrac{1}{2}\Theta\cos\Theta\right]\right\}.$$

The variation of $\epsilon_D^{(c)}$ with Θ is illustrated in Table 1 and Figure 7. It is apparent that for the case $\Theta = 0$, $\epsilon_D^{(c)} = 1$; this gives the well-known result for the drag of a flat plate normal to a hyperthermal flow. C_H has in fact proved to be independent of Θ, the result being identical to that for a flat plate (or, for that matter, any non-concave body) having the same frontal area. This is entirely to be expected, since in a hyperthermal flow the total number of incident free-stream molecules per unit time, which is equal to the total number reflected completely away from the surface per unit time, is dependent upon frontal area only for given values of U_∞ and ρ_∞. The energy yielded up by the incident molecules is a function only of U_∞, while the average energy transported away by the reflected molecules is a function only of T_b for perfect thermal accommodation. Thus the surface configuration nowhere enters into the total heat transfer characteristics.

2.9 The spherical surface

The coordinate system for this surface is defined in Figure 4. We shall consider only the case for which the surface is axially symmetric about the free-stream direction.

We must first determine how Φ in equations (21) varies with ψ. Now

$$BC = \frac{r(\cos\theta - \cos\Theta)}{\cos(\theta-\psi)}\cot\Phi \qquad (32)$$

But from circular geometry

$$BC^2 = MB.BN = r^2\sin^2\Theta - OB^2 \qquad (33)$$

$$= r^2\sin^2\Theta - r^2\{(\cos\theta - \cos\Theta)\tan(\theta-\psi) - \sin\theta\}^2$$

yielding finally, from equations (32) and (33),

$$\cot^2\Phi = \frac{\cos^2(\theta-\psi)}{(\cos\theta - \cos\Theta)^2}\left[\sin^2\Theta - \left\{(\cos\theta - \cos\Theta)\tan(\theta-\psi) - \sin\theta\right\}^2\right] \tag{34}$$

Once again the analysis is restricted to cases for which $0 \leq \Theta \leq \pi/2$ so that no part of the surface is shielded from the free-stream.

The Clausing equation for the spherical surface has the constant kernel

$$K_2 = \frac{\cos\delta_1\cos\delta_2}{\pi r_{12}^2} = \frac{1}{4\pi r^2},$$

and hence,

$$N_i(\theta_1) = N_\infty(\theta_1) + \int_0^{2\pi}\int_0^{\Theta} \frac{1}{4\pi r^2}\, N_i(\theta_2)\, .\, r^2\sin\theta_2 d\theta_2 d\zeta .$$

Since from the axisymmetry of the configuration N_i is a function of θ alone, we may carry out the integration over ζ to obtain

$$N_i(\theta_1) = n_\infty U_\infty \cos\theta_1 + \tfrac{1}{2}\int_0^{\Theta} \sin\theta_2\, N_i(\theta_2) d\theta_2 . \tag{35}$$

The solution of the equation is best found by multiplying by $\sin\theta_1$ and integrating with respect to θ_1

$$\int_0^{\Theta} N_i(\theta_1)\sin\theta_1 d\theta_1 = n_\infty U_\infty \int_0^{\Theta}\sin\theta_1\cos\theta_1 d\theta_1 + \tfrac{1}{2}\int_0^{\Theta}\sin\theta_1 d\theta_1 \int_0^{\Theta}\sin\theta_2 N_i(\theta_2) d\theta_2$$

Thus

$$\int_0^{\Theta} N_i(\theta_2)\sin\theta_2 d\theta_2 = 2n_\infty U_\infty \sin^2\tfrac{1}{2}\Theta ,$$

and

$$N_i(\theta) = n_\infty U_\infty(\cos\theta + \sin^2\tfrac{1}{2}\Theta), \tag{36}$$

the contribution due to reflections being constant over the surface. Equations (21) and (36) now lead to

$$C_D = 2 + \epsilon_D^{(s)}(\Theta)\,\frac{\sqrt{\pi}}{S}\sqrt{\frac{T_b}{T_\infty}},$$

$$C_L = 0, \qquad (37)$$

$$C_H = 1 - \epsilon_H^{(s)}(\Theta)\cdot\tfrac{1}{2}\left(\frac{\gamma+1}{\gamma-1}\right)\frac{T_b}{T_\infty}\cdot\frac{1}{S^2},$$

where

$$\epsilon_D^{(s)} = \frac{6}{\pi\sin^2\Theta}\int_0^{\Theta}\int_{-\Psi}^{\Psi_2}(\cos\theta+\sin^2\tfrac{1}{2}\Theta)\cos\psi\cos(\theta-\psi)\{\cos\Phi-\tfrac{1}{3}\cos^3\Phi\}\sin\theta\,d\psi\,d\theta$$

$$\epsilon_H^{(s)} = \frac{1}{\pi\sin^2\Theta}\int_0^{\Theta}\int_{-\Psi_1}^{\Psi_2}(\cos\theta+\sin^2\tfrac{1}{2}\Theta)\cos\psi\{\pi-2\Phi+\sin2\Phi\}\sin\theta\,d\psi\,d\theta.$$

The coefficients are made dimensionless with respect to the base area $\pi r^2\sin^2\Theta$. Here Φ is given by equation (34), and the limits on ψ are, as in the cylindrical case,

$$\Psi_2 = \tfrac{1}{2}(\pi - \Theta + \theta)$$

$$-\Psi_1 = -\tfrac{1}{2}(\pi - \Theta - \theta)$$

C_L vanishes owing to the axisymmetry of the problem. Since the expressions above cannot be integrated analytically they were evaluated numerically using a Ferranti Pegasus computer. The variations of $\epsilon_D^{(s)}$ and $\epsilon_H^{(s)}$ with Θ are portrayed in Table II and Figure 8, and it will be noted that $\epsilon_H^{(s)}$ is found to differ by less than 0.1% from unity over the entire range of Θ, whereas in fact its value must be exactly unity, as previously explained (Section 2.8). This affords some indication as to the accuracy to be expected in the calculated values of $\epsilon_D^{(s)}$.

2.10 Extension of cylindrical surface theory - the L/D characteristics of cambered plates

The theory of the cylindrical surface is now extended to include cases where the chord is not normal to the flow (see Figure 5). In

order that no part of the surface is shielded from the free-stream we must impose the restriction $\Theta \leq \alpha$, where α is the angle of incidence. The limits on θ are now $(\pi/2 - \alpha + \Theta)$ and $(\pi/2 - \alpha - \Theta)$. It is in fact found simpler to work in terms of $\alpha^* = \pi/2 - \alpha$; we obtain for the limits on ψ

$$\Psi_2 = \tfrac{1}{2}(\pi - \Theta - \alpha^* + \theta)$$

$$-\Psi_1 = -\tfrac{1}{2}(\pi - \Theta + \alpha^* - \theta)$$

giving from equations (22)

$$D = A_B \rho_\infty U_\infty^2 + \frac{RT_b}{2\pi} \int_{\alpha^* - \Theta}^{\alpha^* + \Theta} \rho_r(\theta)\{(\pi - \Theta)\cos\theta + \cos\alpha^* \sin\Theta\} r d\theta$$

$$L = \frac{RT_b}{2\pi} \int_{\alpha^* - \Theta}^{\alpha^* + \Theta} \rho_r(\theta)\{(\pi - \Theta)\sin\theta + \sin\alpha^* \sin\Theta\} r d\theta \qquad (38)$$

$$\dot{Q} = \tfrac{1}{2} A_B \rho_\infty U_\infty^3 - \pi \left(\frac{\gamma+1}{\gamma-1}\right) \left(\frac{RT_b}{2\pi}\right)^{3/2} \int_{\alpha^* - \Theta}^{\alpha^* + \Theta} \rho_r(\theta) \cos\tfrac{1}{2}\Theta \cos\tfrac{1}{2}(\theta - \alpha^*) r d\theta .$$

The equation for the variation of molecular flux over the surface is identical with equation (24), except that the limits on the integral term become $\alpha^* \pm \Theta$. It is solved similarly, the result of this somewhat tedious process being

$$N_i(\theta) = n_\infty U_\infty \left[\tfrac{3}{4}\cos\theta - \frac{\frac{1}{4}\sin\alpha^* \cos^3\tfrac{1}{2}\Theta}{(\cos\tfrac{1}{2}\Theta + \tfrac{1}{2}\Theta \sin\tfrac{1}{2}\Theta)}(\theta - \alpha^*) + \tfrac{1}{4}\cos\alpha^*(2 - \cos\Theta) \right] \qquad (39)$$

Equation (12) now gives $\rho_r(\theta)$, which is substituted into equation (38). Integration and reduction to coefficient form with respect to the chord $2r\sin\Theta$ yield

$$C_D = 2\sin\alpha + \epsilon_D^{(c)}(\Theta, \alpha) \frac{\sqrt{\pi}}{S} \sqrt{\frac{T_b}{T_\infty}} \sin^2\alpha$$

$$C_L = \epsilon_L^{(c)}(\Theta) \frac{\sqrt{\pi}}{S} \sqrt{\frac{T_b}{T_\infty}} \sin\alpha\cos\alpha \qquad (40)$$

$$C_H = \sin\alpha \left(1 - \tfrac{1}{2}\left(\frac{\gamma+1}{\gamma-1}\right) \frac{T_b}{T_\infty} \cdot \frac{1}{S^2}\right)$$

where

$$\epsilon_D^{(c)} = \frac{1}{2\pi\sin^2\alpha}\left\{(\pi-\Theta)\left[\frac{3}{4}\left(\frac{\Theta}{\sin\Theta} - \cos\Theta\right) + \sin^2\alpha(\cos\Theta + 1)\right.\right.$$

$$\left. - \frac{\frac{1}{2}\cos^2\alpha\cos^3\frac{1}{2}\Theta}{\left(\cos\frac{1}{2}\Theta + \frac{1}{2}\Theta\sin\frac{1}{2}\Theta\right)}\left(\frac{\Theta\cos\Theta}{\sin\Theta} - 1\right)\right]$$

$$\left. + \sin^2\alpha\left[\frac{3}{2}\sin\Theta + \frac{1}{2}\Theta(2 - \cos\Theta)\right]\right\}$$

and

$$\epsilon_L^{(c)} = \frac{1}{2\pi}\left\{(\pi-\Theta)\left[(\cos\Theta + 1) + \frac{\frac{1}{2}\cos^3\frac{1}{2}\Theta}{\left(\cos\frac{1}{2}\Theta + \frac{1}{2}\Theta\sin\frac{1}{2}\Theta\right)}\left(\frac{\Theta\cos\Theta}{\sin\Theta} - 1\right)\right]\right.$$

$$\left. + \left[\frac{3}{2}\sin\Theta + \frac{1}{2}\Theta(2 - \cos\Theta)\right]\right\}$$

Once again C_H is found to be dependent on frontal area only. The factors $\epsilon_D^{(c)}$ and $\epsilon_L^{(c)}$ are chosen to refer C_D and C_L to the standard results for a flat plate at the same incidence, namely

$$C_D = 2\sin\alpha + \frac{\sqrt{\pi}}{S}\sqrt{\frac{T_b}{T_\infty}}\sin^2\alpha$$

$$C_L = \frac{\sqrt{\pi}}{S}\sqrt{\frac{T_b}{T_\infty}}\sin\alpha\cos\alpha$$

The variations of $\epsilon_D^{(c)}$ and $\epsilon_L^{(c)}$ with α and Θ are shown in Figures 9 and 10, while the variations of C_D, C_L and C_L/C_D are portrayed in Figures 11, 12, 13 and 14 and Table III for various values of α, Θ and $\frac{\sqrt{\pi}}{S}\sqrt{\frac{T_b}{T_\infty}}$.

2.11 Coefficients of local heat transfer for concave surfaces

At any point on a concave surface the three contributions to the heat transfer are:

(i) Incidences of free-stream molecules, each transporting a total energy $e_\infty(U_\infty)$.

(ii) Incidences of molecules which have been multiply reflected, each carrying an average total energy $e_b(T_b)$.

(iii) Reemissions of molecules from the surface, these molecules also carrying average total energy $e_b(T_b)$.

The local heat transfer rate is therefore, per unit area,

$$E(\underline{\xi}) = N_\infty(\underline{\xi})e_\infty + N_b(\underline{\xi})e_b - N_r(\underline{\xi})e_b$$

However, since $N_i(\underline{\xi}) = N_r(\underline{\xi})$ we have by virtue of equation (1)

$$E(\underline{\xi}) = N_\infty(\underline{\xi})e_\infty + N_b(\underline{\xi})e_b - N_\infty(\underline{\xi})e_b - N_b(\underline{\xi})e_b$$

$$= N_\infty(\underline{\xi})\,(e_\infty - e_b) \qquad (41)$$

But this is precisely the result which holds for non-concave surfaces, and it arises because of our assumption of perfect thermal accommodation at the surface. With this assumption an impact and subsequent reemission of a multiply reflected molecule leads to no net transfer of energy.

We see thus that the heat transfer characteristics of a concave surface are identical with those of the corresponding convex surface, the local heat transfer coefficient being given by the standard result

$$C'_H(\underline{\xi}) = \frac{E(\underline{\xi})}{\frac{1}{2}\rho_\infty U_\infty^3} = \left(1 - \tfrac{1}{2}\left(\frac{\gamma+1}{\gamma-1}\right)\frac{T_b}{T_\infty}\cdot\frac{1}{S^2}\right)\cos\beta \qquad (42)$$

where β is the angle between the free-stream direction and the normal to the surface at $\underline{\xi}$.

3. Discussion of results

3.1 The effects of surface temperature and speed ratio

It is apparent from equations (31), (37) and (40) that the reflection contributions to C_D, C_L (which is entirely governed by reflections) and C_H are proportional to the parameter $\frac{1}{S}(T_\infty/T_b)^{\frac{1}{2}}$. The lift in particular, therefore, will be strongly influenced by variations in this quantity.

We are restricted by the hyperthermal approximation to values of $S > 6$, and investigations of the upper atmosphere by means of satellite observations have revealed that daytime values of T_∞ vary from $\sim 1200°K$ at an altitude of 200km to $\sim 2000°K$ at 600km. These figures are very

approximate, being subject to large diurnal fluctuations and to considerable uncertainty due to the difficulty of the measurements (16). The surface temperature may be found by setting up and solving an energy balance equation, using the heat transfer characteristics already determined, and taking into account the effects of radiation. However, this problem contains a great many variables, and satellite measurements indicate that the surface temperature of bodies in the free molecule flow region remains at about 300°K. Thus a figure of 0.4 - 0.5 for $(T_b/T_\infty)^{\frac{1}{2}}$ is realistic, leading to a maximum value for $\frac{1}{S}(T_b/T_\infty)^{\frac{1}{2}}$ of ~ 0.1 for most applications operating in this region. Figure 14 shows the important effect of $\frac{1}{S}(T_b/T_\infty)^{\frac{1}{2}}$ in determining the L/D characteristics of a flat plate in free-molecule flow; this form of variation is typical also of the curved surfaces studied.

3.2 The effect of surface geometry on aerodynamic forces

We consider first those cases which give rise solely to a drag force (Sections 2.8, 2.9; Figures 7 and 8). The drag of the surface is determined by the balance between two conflicting processes. Firstly, the effect of concavity is to channel the outgoing momentum, so that from any point on the surface those molecules which escape completely all carry a momentum component contrary to the free-stream direction. In contrast, the corresponding convex surface permits a certain proportion of molecules to escape in such directions that they carry momentum components travelling with the free-stream. The channelling of reflected momentum by the concave surface leads to an increase in the reflection drag. The second effect of concavity is to redistribute the incident molecular flux over the surface, the increase in flux due to the multiple reflections being proportionately greater on those parts of the surface at low local incidences to the flow. Since Lambert's law is assumed to hold, most molecules are emitted in directions nearly perpendicular to the surface, and hence a greater proportion of molecules are emitted in directions nearly normal to the flow than would be the case in the absence of multiple reflection, leading to a corresponding decrease in the reflection drag. The factors $\epsilon_D^{(c)}$ in equation (31a) and $\epsilon_D^{(s)}$ in equation (37a) are both in fact found to be in excess of 1 (Figures 7 and 8); the surfaces thus have reflection drag exceeding that of a flat plate normal to the flow, for which $\epsilon_D = 1$, and the first of the effects described above predominates.

The maximum possible drag coefficient for a concave surface would occur if this channelling process could be taken to its logical extreme and all the emitted molecules were constrained to travel exactly in opposition to the free-stream motion. The average velocity of molecules emitted diffusely at temperature T_b is $^3/_4\sqrt{2\pi RT_b}$, leading to a value of 1.5 for $\epsilon_{D_{max}}$. Possibly surfaces having a considerably greater degree of concavity than those studied here may prove to have values of ϵ_D approaching this maximum.

Figures 7 and 8 show that the maximum reflection contributions to the drag coefficients of the two surfaces studied are larger than that for the flat plate normal to the flow by ~ 3% for the cylindrical surface and ~ 5% for the spherical surface. For a realistic value of $\frac{1}{S}(T_b/T_\infty)^{\frac{1}{2}}$ the reflection contribution is in any case small (less than ~ 10%), and increments thereto of this order are unlikely to have any practical significance.

Turning now to cases involving lift forces (Section 2.11, Figures 9-14 and Table III) it is found that once again the drag is substantially independent of concavity for practical values of $\frac{1}{S}(T_b/T_\infty)^{\frac{1}{2}}$ (Figure 11). The flat plate is seen to generate the most lift at a given incidence, the value of C_L falling off as Θ increases. For $\Theta = \pi/10$ we have a reduction in lift of ~ 3% over the flat plate value, and for higher curvatures the lift falls off rapidly. Maximum lift is developed at an incidence of 45°, independent of curvature.

The L/D ratio (Figure 13) is largest at low incidences, the highest value obtained being that for the flat plate at incidences approaching zero, although the hyperthermal approximation is not strictly valid for very low incidences since the molecular thermal velocities are not necessarily negligible in comparison with the free-stream velocity component normal to the surface. Of the surfaces examined, the flat plate is plainly the most efficient as far as the generation of lift is concerned, but with $\frac{1}{S}(T_b/T_\infty)^{\frac{1}{2}} \leq 0.1$ the maximum attainable L/D ratios are none the less very small (Figure 14). One cannot in fact expect much aerodynamic lift in the free-molecule flow regime, and in practice speeds must be high enough to generate substantial centrifugal lift in the earth's gravitational field in order to sustain any vehicle at such extreme altitudes.

It must be borne in mind that the theoretical analysis has been restricted to those instances in which no part of the concave surface is shielded from the free-stream; the necessary condition is that $\alpha \geq \Theta$. For lower incidences impacts of free-stream molecules will occur on the convex upper surface, giving rise to a negative lift component. The shielding also leads to a reduction in molecular flux over the lower surface, with a consequent further diminution in total lift. Thus although the L/D ratio increases with decreasing incidence until the condition $\alpha = \Theta$ is reached, it falls off markedly with further decrease in incidence, being entirely negative for zero incidence.

3.3 Comparison with results obtained by Chahine

In his papers (6,7) Chahine has presented an analysis of both the infinite cylindrical surface and the spherical surface. His approach to the problem is in principle similar to that employed here, though

throughout he considers the three contributions due to the incident free-stream molecules, the incident inter-reflected molecules, and the emitted molecules, separately at each point on the surface (as in equation (6) of this report). Rather greater generality is achieved in the treatment of the energy transfer, however, by the introduction of partial surface accommodation. The thermal accommodation coefficient is assumed to be constant over the surface, the distribution of incident energy over the surface being found from an equation analogous to the Clausing equation for the distribution of molecular flux. This equation has the form

$$E_i(\underline{\xi}_1) = \eta(E_\infty(\xi_1),\ T_b,\ \alpha') + \int_\Sigma (1 - \alpha')E_i(\underline{\xi}_2)K(\underline{\xi}_1,\underline{\xi}_2)d\Sigma$$

in which η is a function of the incident free-stream energy, the surface temperature and the accommodation coefficient.

Chahine's results indicate, as do those obtained in the present analysis, that for perfect accommodation the heat transfer coefficient (referred to the base area) is independent of surface geometry. However, the values he obtains for the C_D and C_L of the cylindrical surface do not agree with those derived in Section 2 of this report, he finds, for instance, that the drag of a concave cylindrical surface with chord normal to the flow is less than that of a flat plate at equal incidence, while here it is found to be greater (Figure 7). The source of this discrepancy appears to lie in the last term of the equation (2.35) of Ref. (6), which should contain a factor $\frac{1}{2}$. With this correction Chahine's analysis yields the same results as that employed here. He quotes no numerical results for the drag of the spherical surface, and to obtain one from his paper it appears necessary to evaluate numerically a quadruple integral involving an unwieldy trigonometrical function.

The method developed in Section 2, which considers only the effect of incident free-stream particles and of particles reemitted directly into the free-stream, appears the more suited to the investigation of other classes of concave surfaces, especially in cases of axially symmetric surfaces, since the equations lead to a double integral rather than the quadruple integral resulting from Chahine's method. The task of computation of the coefficients will thus be correspondingly lessened.

4. Conclusions

An examination has been made of the problem of free-molecule flow over concave surfaces. With the assumption of perfectly diffuse molecular reflection with complete accommodation to the surface conditions, general equations have been derived for the lift, drag, and heat transfer characteristics of such surfaces. These equations have been applied to the infinitely long circular cylindrical arc and to a section of a spherical surface for the case of a hyperthermal flow velocity.

The results obtained indicate that the heat transfer characteristics are identical with those of the corresponding convex surfaces, the total heat transfer being independent of the surface configuration. The effects of concavity are found, for the surfaces investigated, to be an increase in drag and a decrease in lift, when compared to a flat plate at the same incidence to the flow. For most practical cases, however, the effect on the total drag is small, amounting to no more than about 1% for the extreme cases considered; the lift developed is more seriously influenced. Of the geometries examined, the most efficient lifting surface proves to be the flat plate, although the L/D ratios which can be achieved under practical conditions are nevertheless very small.

5. Suggestions for further work

Clearly, scope exists for the application of the method developed in this report to the examination of other types of concave surface in free-molecule flow. Cases which may prove amenable to analysis are (a) two flat plates of infinite span at an angle to each other, (b) an infinite rectangular trough, (c) a reentrant cone, and (d) a circular cylinder with a closed end. The chief problem appears to lie in obtaining a solution of the Clausing equation for the molecular flux redistribution. The method could also be extended to yield pitching moments.

Chahine (6,7) has shown how greater generality may be achieved by the introduction of partial surface accommodation; possibly a further type of surface interaction recently proposed by Schamberg (17) could be employed in a future analysis, to include the effects of imperfectly diffuse reflection. At velocities too low for the hyperthermal approximation to remain valid, the application could be attempted of an approximate method due to Schrello (18) which holds down to $S \simeq 1$. At these lower velocities the reflection contributions to the aerodynamic characteristics will be proportionately larger, and the effects of concavity more marked.

In any but the more simple cases the solution of the Clausing equation will pose a severe problem, and it is interesting to note that in an article by Larish (19) an analogy is pointed out between this equation and the integral equation describing the illumination in a space having non-absorbing walls which reflect in accordance with Lambert's law. Larish suggests that the Clausing equation can be solved by means of such an optical analogue, where the incident molecular flux is represented by external light sources. The intensity of illumination over the surface then provides a measure of the emitted molecular flux. The solution for hyperthermal velocities is particularly easy to find, since the model need only be placed in a parallel beam of light. This relatively simple experimental method for determining the molecular flux redistribution would make possible the treatment of more complicated surfaces than could be tackled by purely theoretical means.

Acknowledgement

The author wishes to express his thanks to Mr. E.A. Boyd of the Department of Aerodynamics for proposing the problem, and for his suggestions during the course of the work.

References

1. Zahm, A.F. — Superaerodynamics, J. Franklin Inst., 217, pp. 153-166 (1934).

2. Schaaf, S.A. and Chambré, P.L. — 'Flow of rarefied gases' in 'Fundamentals of Gas Dynamics' (H.W. Emmons, Ed.), Sect. H, pp. 687-739, Princeton Univ. Press, Princeton (1958).

3. Patterson, G.N. — Molecular Flow of Gases, J. Wiley and Sons. (1956).

4. Hurlbut, F.C. — Aerodynamic force coefficient for a generalized control surface in free molecule flow. (Unpublished).

5. Cohen, I.M. — Free molecule flow over non-convex surfaces, A.R.S. Journal, 30, 8, p. 770 (1960).

6. Chahine, M.T. — 'Free molecule flow over non-convex surfaces' in 'Rarefied Gas Dynamics' (L. Talbot, Ed.) Sect. II, p. 209, Academic Press (1961).

7. Chahine, M.T. — Proceedings 11th International Astronautical Congress, Stockholm 1960, Main Sessions, pp. 473-482. Springer-Verlag, Vienna. (1961).

8. Charwat, A.F. — 'Review of rarefied gas aerodynamics', Ch. 8 of 'Current Research in Aeronautical Sciences' (L. Broglio, Ed.), Pergammon Press. (1961).

9. Wiedmann, H. and Trompler, P. — Trans. A.S.M.E. 68, 57 (1946).

10. Roberts, J.K. — Proc. Roy. Soc. A142, 519 (1933).

11.	Hayes, W.D. and Probstein, R.F.	Hypersonic flow theory, Ch. 10, Sect. 1, Academic Press (1959).
12.	Clausing, P.	On the steady flow of very rarefied gases, Physica, 9, p. 65, (1929).
13.	Kennard, E.H.	Kinetic theory of gases, McGraw-Hill (1938).
14.	Ashley, H.	Applications of the theory of free molecule flow to aeronautics. J. Aero. Sci. 16, pp. 95-104, (1949).
15.	Courant, R. and Hilbert, D.	Methods of mathematical physics. Interscience, New York, (1953).
16.	King-Hele, D.G.	Review of earth-satellite orbital studies at R.A.E., 1959-61 and their application to Russian and American satellites. R.A.E. Report No. G.W. 25 (1961).
17.	Schamberg, R.	A new analytic representation of surface interaction for hyperthermal free molecule flow with applications to satellite drag, RAND Corp. Report P.1609 (1958).
18.	Schrello, D.M.	Approximate free molecule aerodynamic characteristics, A.R.S. Journal 30, 8, p. 765, (1960).
19.	Larish, E.	Izvestiia Akademii Nauk SSSR, Otdelenie Tekhnicheskikh Nauk, Mekhanika i Mashinostroenie 3, pp. 117-120 (1960).

Table I

Values of $\epsilon_D^{(c)}(\Theta)$ for the cylindrical surface, chord normal to the flow

H	$\epsilon_D^{(c)}$
0	1.0000
$\pi/20$	1.0000
$\pi/10$	1.0001
$3\pi/20$	1.0005
$\pi/5$	1.0015
$\pi/4$	1.0033
$3\pi/10$	1.0063
$7\pi/20$	1.0107
$4\pi/10$	1.0166
$9\pi/20$	1.0242
$\pi/2$	1.0333

Table II

Values of $\epsilon_D^{(s)}$ and $\epsilon_H^{(s)}$ for the spherical surface, chord normal to the flow

Θ	$\epsilon_D^{(s)}$	$\epsilon_H^{(s)}$
0	1.0000	1.0000
$\pi/20$	0.9999	1.0003
$\pi/10$	1.0000	1.0005
$3\pi/20$	1.0001	1.0006
$\pi/5$	1.0016	1.0006
$\pi/4$	1.0044	1.0006
$3\pi/10$	1.0092	1.0007
$7\pi/20$	1.0164	1.0007
$4\pi/10$	1.0262	1.0007
$9\pi/20$	1.0388	1.0007
$\pi/2$	1.0539	1.0007

The values given here have been obtained by correcting the results of a numerical analysis carried out using the Pegasus computer.

	$\epsilon_L^{(c)}$	$\epsilon_D^{(c)}$										
Θ	all $\alpha \geq \Theta$	$\alpha=\pi/2$	0.45π	0.4π	0.35π	0.3π	0.25π	0.2π	0.15π	0.1π	0.05π	0
0	1.0000	1.0000	1.0000	1.0000	1.0000	1.0000	1.0000	1.0000	1.0000	1.0000	1.0000	1.0000
0.05π	0.9922	1.0000	1.0002	1.0008	1.0020	1.0041	1.0078	1.0148	1.0300	1.0738	1.3105	
0.1π	0.9709	1.0001	1.0008	1.0032	1.0077	1.0155	1.0293	1.0555	1.1127	1.2770		
0.15π	0.9394	1.0005	1.0020	1.0070	1.0164	1.0328	1.0616	1.1163	1.2360			
0.2π	0.9013	1.0015	1.0040	1.0120	1.0275	1.0543	1.1016	1.1912				
0.25π	0.8602	1.0033	1.0069	1.0184	1.0404	1.0788	1.1464					
0.3π	0.8195	1.0063	1.0110	1.0260	1.0548	1.1049						
0.35π	0.7817	1.0107	1.0164	1.0349	1.0701							
0.4π	0.7490	1.0166	1.0233	1.0449								
0.45π	0.7227	1.0242	1.0317									
0.5π	0.7037	1.0333										

Table III

The variation of $\epsilon_L^{(c)}$ and $\epsilon_D^{(c)}$ with α and Θ.

Values of C_L and C_D are obtained by substitution of $\epsilon_L^{(c)}$ or $\epsilon_D^{(c)}$ into equations (40).

CONFIGURATION FOR DETERMINATION OF THE KERNEL IN THE CLAUSING INTEGRAL EQUATION (3)

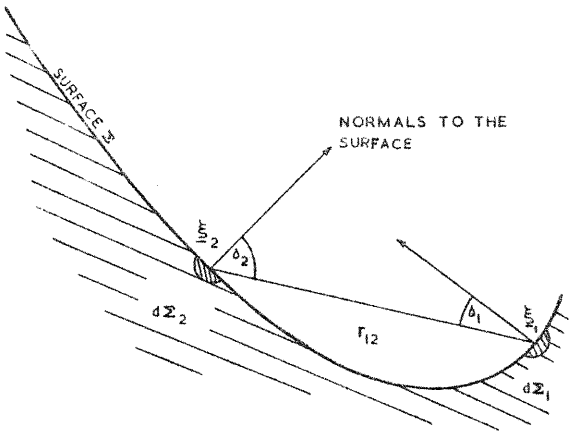

FIG. 1.

COORDINATE SYSTEM AT A POINT $\underline{\xi}$ ON THE SURFACE

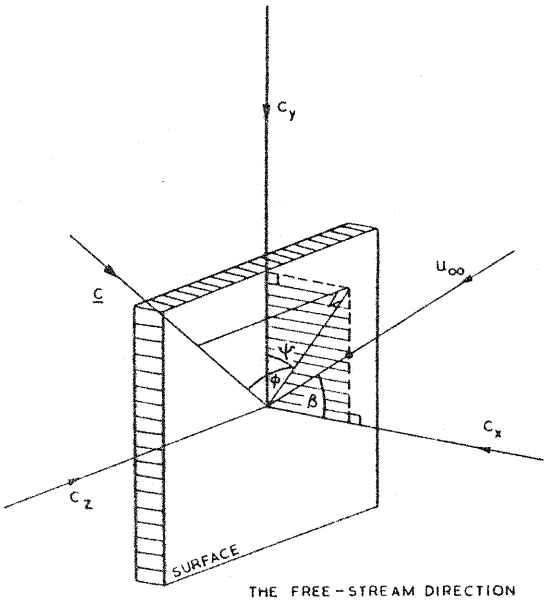

THE FREE-STREAM DIRECTION IS CONTAINED BY THE xy-PLANE

FIG. 2.

CYLINDRICAL ARC SURFACE - NON LIFTING CASE.

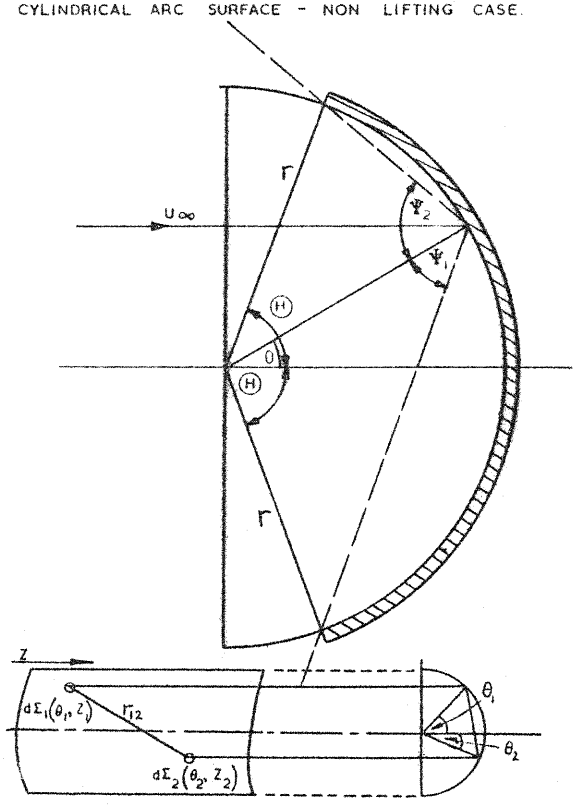

FIG. 3

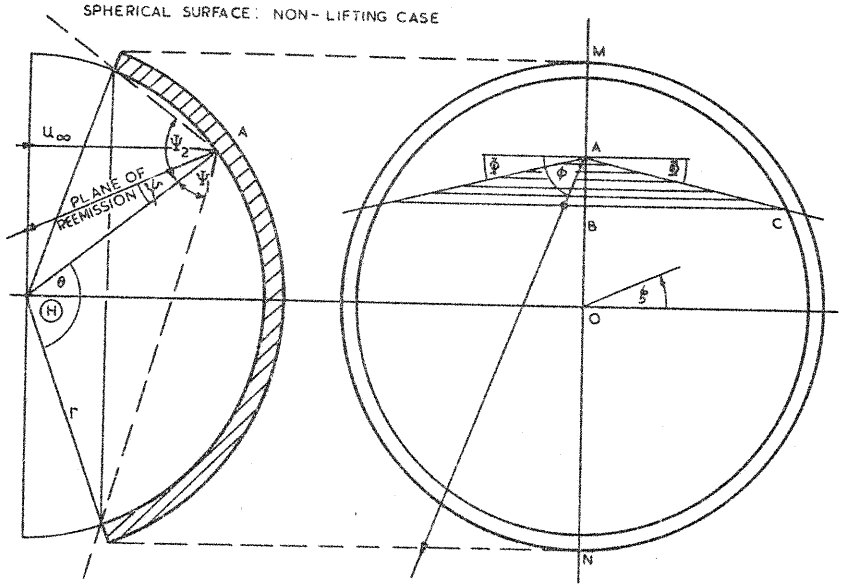

FIG. 4.

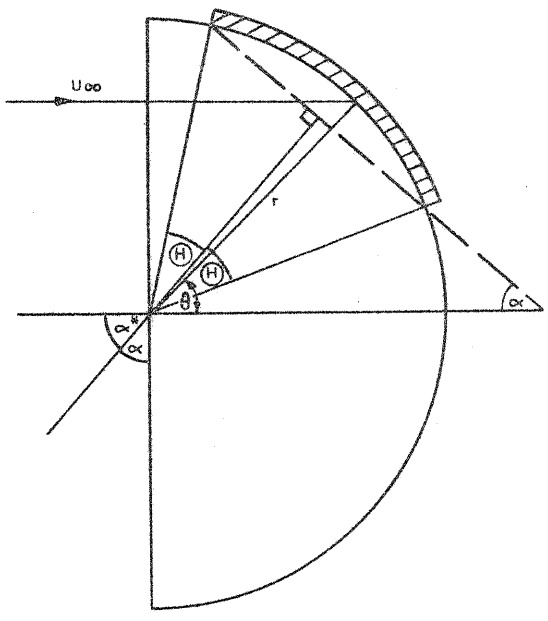

CYLINDRICAL ARC SURFACE. LIFTING CASE

FIG. 5.

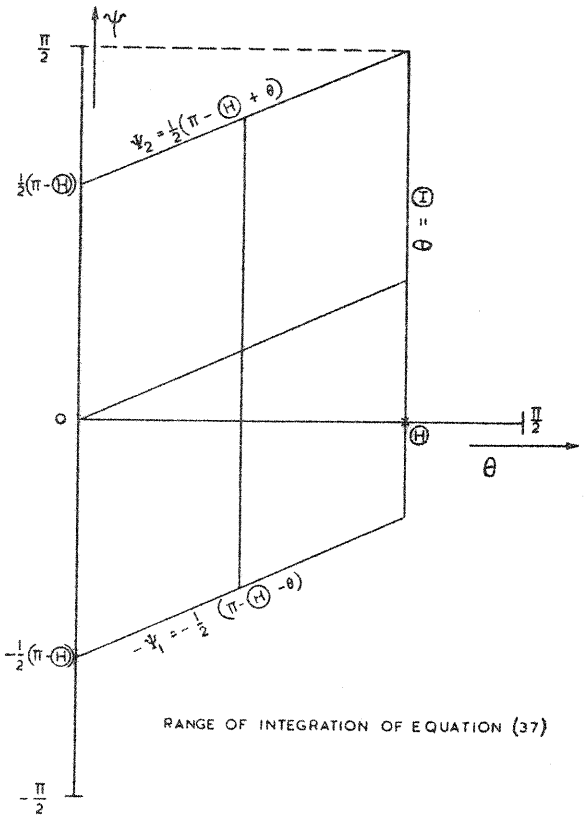

RANGE OF INTEGRATION OF EQUATION (37)

FIG. 6.

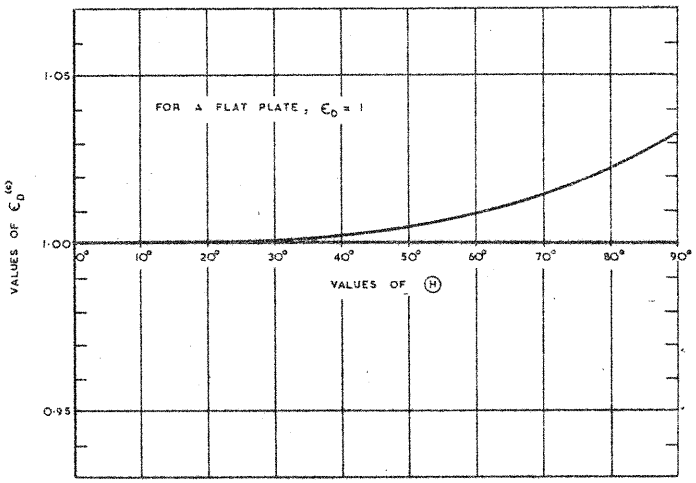

FIG. 7. CYLINDRICAL ARC SURFACE, CHORD NORMAL TO THE FLOW

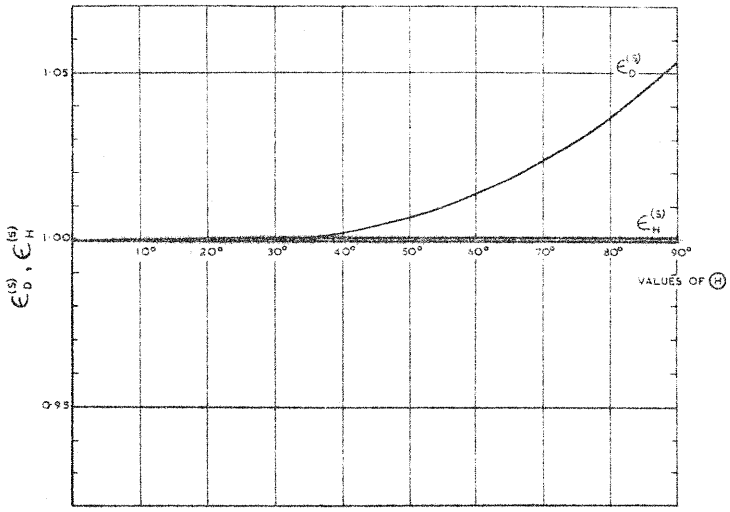

FIG 8. SPHERICAL SURFACE, CHORD NORMAL TO THE FLOW.

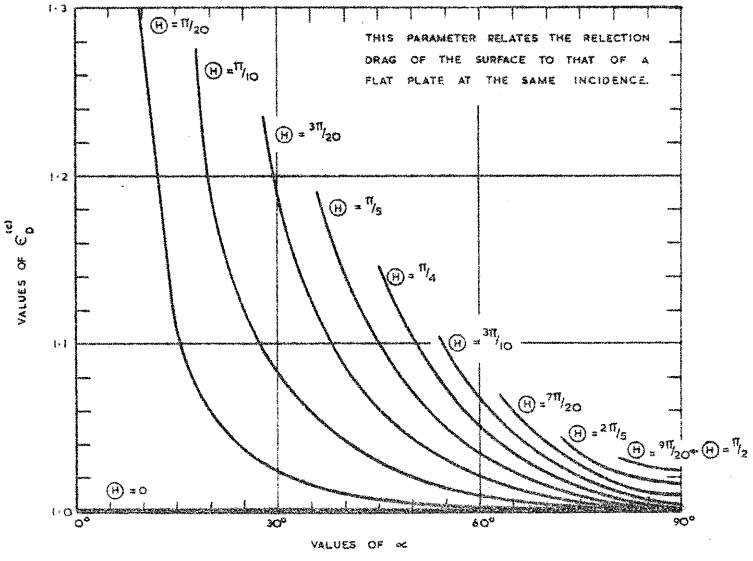

FIG. 9. VARIATIONS OF $\epsilon_D^{(c)}$ WITH Ⓗ AND ∝

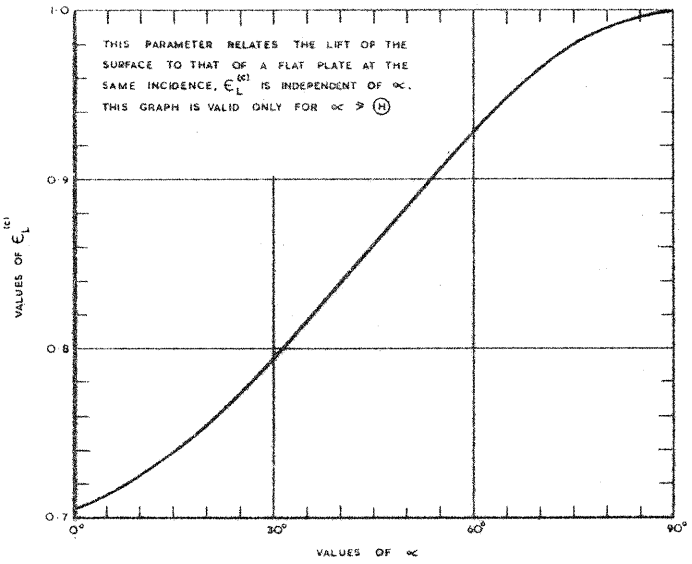

FIG. 10. VARIATION OF $\epsilon_L^{(c)}$ WITH (H)

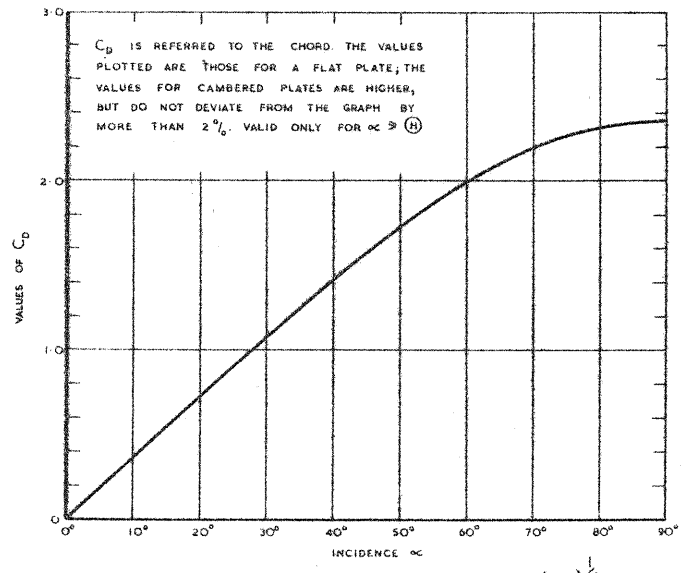

FIG.11. C_D FOR CYLINDRICALLY CAMBERED PLATES WITH $\frac{1}{S}\left(\frac{T_b}{T_\infty}\right)^{1/2} = 0 \cdot 2$

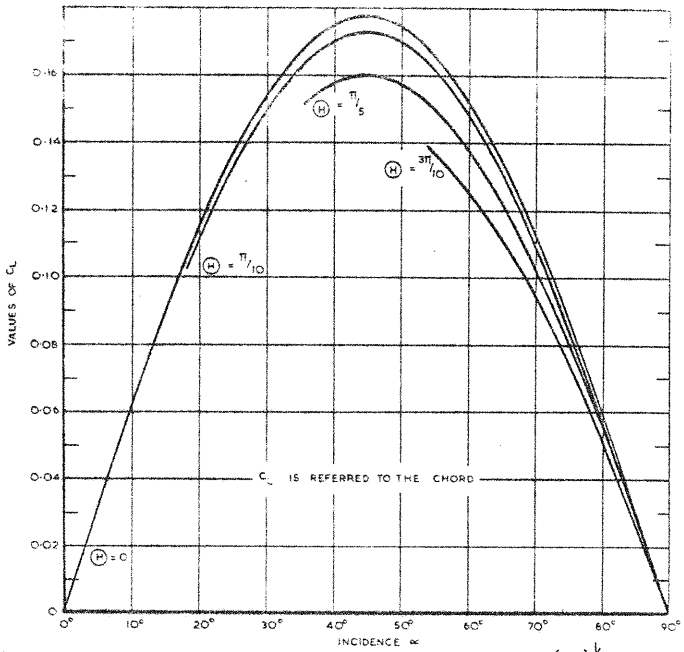

FIG. 12. C_L OF CYLINDRICALLY CAMBERED PLATES FOR $\frac{1}{S}\left(\frac{T_b}{T_\infty}\right)^{1/2} = 0{\cdot}2$

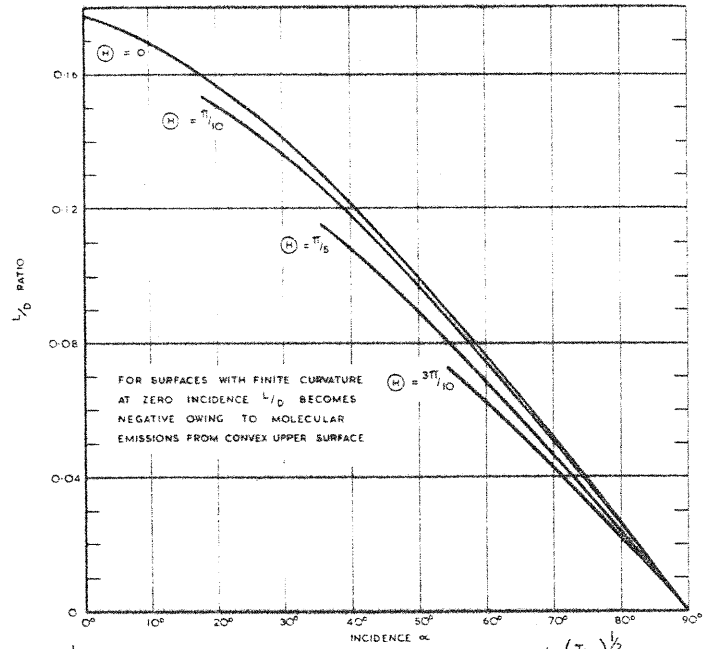

FIG. 13. L/D RATIO OF CYLINDRICALLY CAMBERED PLATES FOR $\frac{1}{S}\left(\frac{T_b}{T_\infty}\right)^{1/2} = 0{\cdot}2$

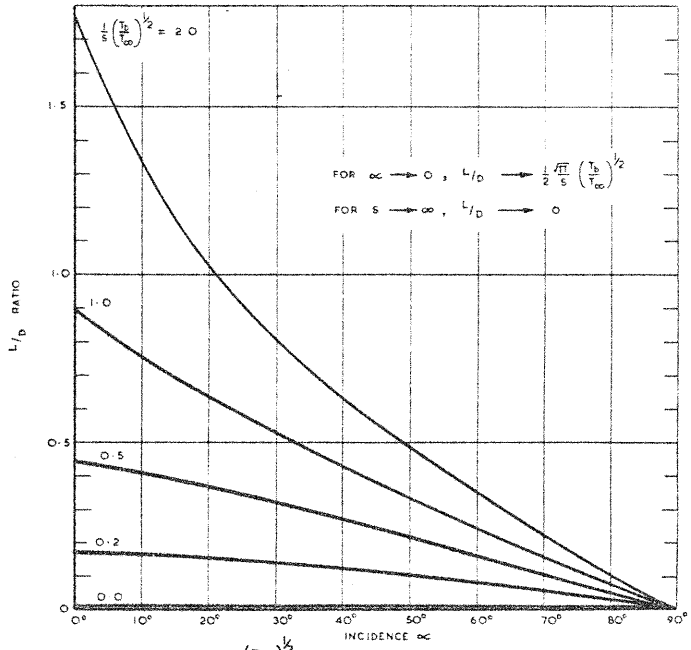

FIG. 14. EFFECT OF $\frac{1}{S}\left(\frac{T_b}{T_\infty}\right)^{1/2}$ ON L/D FOR A FLAT PLATE.